

SLAC-PUB-10710
September 2004

Electron Cloud Effect in the Linear Colliders

M. Pivi and T. Raubenheimer

Stanford Linear Accelerator Center, Stanford University, Stanford, CA 94309

Published in ICFA Beam Dyn. Newslett. 33:64-70, 2004

Work supported by the Department of Energy contract DE-AC02-76SF00515.

1.1 Electron Cloud effect in the Linear Colliders

Published in ICFA Beam Dyn. Newslett. 33:64-70, 2004

M. Pivi mpivi@slac.stanford.edu SLAC, Menlo Park, California 94025, US
T. Raubenheimer tor@slac.stanford.edu SLAC, Menlo Park, California 94025, US

1.1.1 Introduction

Beam induced multipacting, driven by the electric field of successive positively charged bunches, may arise from a resonant motion of electrons, generated by secondary emission, bouncing back and forth between opposite walls of the vacuum chamber. The electron-cloud effect (ECE) has been observed or is expected at many storage rings [1].

In the beam pipe of the Damping Ring (DR) of a linear collider, an electron cloud is produced initially by ionization of the residual gas and photoelectrons from the synchrotron radiation. The cloud is then sustained by secondary electron emission. This electron cloud can reach equilibrium after the passage of only a few bunches. The electron-cloud effect may be responsible for collective effects as fast coupled-bunch and single-bunch instability, emittance blow-up or incoherent tune shift when the bunch current exceeds a certain threshold, accompanied by a large number of electrons in the vacuum chamber.

The ECE was identified as one of the most important R&D topics in the International Linear Collider Report [2]. Systematic studies on the possible electron-cloud effect have been initiated at SLAC for the GLC/NLC and TESLA linear colliders, with particular attention to the effect in the positron main damping ring (MDR) and the positron Low Emittance Transport which includes the bunch compressor system (BCS), the main linac, and the beam delivery system (BDS). We present recent computer simulation results for the main features of the electron cloud generation in both machine designs. Thus, single and coupled-bunch instability thresholds are estimated for the GLC/NLC design.

The results are obtained by the computer simulation codes POSINST vers. 12, HEAD-TAIL vers. 02/04 and CLOUD_MAD vers. 2.3, which were developed at LBNL, CERN and SLAC [3,4,5] respectively, to study the electron-cloud effect in particle accelerators. The former code is used to simulate the electron cloud generation, to estimate the equilibrium electron-cloud density and to estimate the coupled bunch instability, while the latter two codes are used to estimate the single-bunch head-tail instability and the emittance growth. Electron-cloud studies for CLIC are discussed in [6].

The GLC/NLC MDR stores 3 trains, separated by 65 nsec with each train consisting of 192 bunches having 1.4 nsec bunch spacing. The aluminum vacuum chamber is specified to be a cylindrical perfectly-conducting round pipe with a 20 mm radius and includes an antechamber to remove most of the synchrotron radiation. The TESLA main damping ring stores 2820 bunches with a 20 nsec bunch spacing. The vacuum chamber in the long straight sections is a round aluminum pipe with a 50 mm radius without an antechamber. The arc vacuum chambers are assumed to be round

chambers without an ante-chamber and with 22 mm radius. The TESLA bunch spacing in the linac increases to 337 nsec from the 20 nsec in the damping ring. A complete set of parameters assumed for the simulations can be found in [2,7,8].

In the following, the present status of the studies on the electron cloud generation and effects in the linear colliders will be described. In general, the electron cloud effects are so severe that the generation of a cloud in a significant fraction of the rings or beam lines will have deleterious effects. Finally, possible remedies to mitigate the effect are presented.

1.1.2 Generation of the cloud

The simulation code POSINST for the generation of the electron cloud and the detail model of the secondary electron yield (SEY or δ) are described in [9,10]. The code offers the possibility of simulating multiple field configurations including solenoid, arc dipole, quadrupole, sextupole and wigglers sections and includes a model for the fringe fields ends.

The secondary electron yield, number of secondary electrons generated, is a function of the primary incident electron energy and angle and, together with the secondary electron energy, is the key parameter for the electron-cloud effect. The main SEY parameters are the peak SEY value δ_{\max} and secondary emitted-electron energy spectrum $d\delta/dE$.

Typically the electron-cloud develops under the conditions where the average SEY of the electrons hitting the wall is larger than one. The cloud develops until an equilibrium electron density level is reached which arises due to a balance between the space charge forces, the beam potential well, and the rate of electron generation. The equilibrium density level is typically close to the neutralization level which is defined as the point where the average number of electrons equals the average number of positively charged particles. In the damping rings, the neutralization level is typically between $4.0E+11$ and $1.0E+13$ e/m³ depending on the beam intensity and vacuum chamber sizes. In these studies, we are mainly interested in the estimate of the equilibrium electron density as a function of the peak value of the SEY.

1.1.3 Thresholds for the development of the cloud: SEY Thresholds

The typical peak SEY for *as received* aluminum 6063 technical vacuum chamber material is ~ 2.7 . Simulation results for the GLC/NLC main damping rings [10] indicate that the secondary electron yield threshold for the development of the electron-cloud is $\delta_{\max} = 1.6$ in field free regions, and 1.4, 1.3, and 1.25, respectively in the arc dipole, wiggler and arc quadrupole sections of the GLC/NLC main damping ring. See table I.

Simulations for the TESLA positron damping ring suggest that the electron cloud develops in the long straight sections when $\delta_{\max} > 2.1$. This threshold appears to be safe, however, a serious issue is the multipacting in the ~ 400 m long damping wigglers. In the wiggler sections the vacuum chamber size are smaller and as a consequence the multipacting conditions are enhanced, resulting in a electron-cloud threshold given by $\delta_{\max} = 1.3$, see Fig1.

Furthermore, the TESLA damping ring arcs vacuum chamber design actually does not include an antechamber. Without an antechamber, the synchrotron radiation generates a large amount of photoelectrons at the wall and the electron-cloud is present independently of the SEY. In our simulations, we have also considered the possibility to include an antechamber design and switched off the synchrotron radiation. In this case, in the arc quadrupoles and dipoles the thresholds are given by $\delta_{\max} = 1.6, 1.5$, respectively.

Therefore to avoid the detrimental effect given by the electron-cloud in the damping rings, a SEY as low as 1.2 needs to be achieved in at least the damping wiggler sections of either ring design machines. The aim is to reduce the SEY of the vacuum chamber material below the specified thresholds.

Studies have also been made of the electron cloud generation in the positron transport lines. This is only expected to be an issue in the normal conducting colliders where the bunches are closely spaced while, in the TESLA design, the bunch spacing is 337 ns after extraction from the damping ring. In the GLC/NLC transport lines, the peak electron cloud density is a strong function of the vacuum chamber radius as well as the SEY. Assuming the worst case of a 1 cm chamber radius and an SEY = 2, the cloud density grew to the neutralization level of $6E+13 \text{ e/m}^3$. However, decreasing the SEY to 1.5 or increasing the vacuum chamber radius to 2 cm decreased the peak cloud density to $2E+11 \text{ e/m}^3$. Further decreases were seen with addition reduction of the SEY or increase of the chamber aperture however the electron cloud due to the photo-electrons must still be estimated. An ante-chamber in the bunch compressor arcs and the BDS arcs may be required to keep the photo-electrons at a sufficiently low level.

Table I. Secondary electron yield thresholds for the development of the electron-cloud in the GLC/NLC and TESLA DRs. The TESLA damping ring arcs vacuum chamber design does not include an antechamber. Without an antechamber and assuming a photoelectron yield of 10%, the photoelectrons dominate and an electron-cloud is present independent of the SEY.

Damping Ring location	Parameters	δ_{\max} threshold	neutralization Cloud density
GLC/NLC field free region		1.5÷1.6	$2E13 \text{ m}^{-3}$
“ arc dipole	$B_y=0.675 \text{ T}$	1.3÷1.4	$2E13 \text{ m}^{-3}$
“ arc quadrupole	$G=30 \text{ T/m}$	1.2÷1.25	$2E13 \text{ m}^{-3}$
“ damping wiggler	$B_y=2.1 \text{ T}, \lambda_w=0.27\text{m}$	1.2÷1.3	$6E13 \text{ m}^{-3}$
TESLA long straight sections		2.0÷2.1	$4E11 \text{ m}^{-3}$
“ arc dipole without antechamber	$B_y=0.194 \text{ T}$	Photo e^-	$2E12 \text{ m}^{-3}$
“ arc dipole with antech.	$B_y=0.194 \text{ T}$	1.4÷1.5	$2E12 \text{ m}^{-3}$
“ arc quadrupole without antechamber	$G=21.7 \text{ T/m}$	Photo e^-	$2E12 \text{ m}^{-3}$
“ arc quadrupole with antechamber	$G=21.7 \text{ T/m}$	1.5÷1.6	$2E12 \text{ m}^{-3}$
“ damping wiggler	$B_y=1.6 \text{ T}, \lambda_w=0.4\text{m}$	1.2÷1.3	$5E12 \text{ m}^{-3}$

1.1.4 Head-Tail single-bunch and coupled bunch instabilities

We have estimated the electron cloud density threshold for the head-tail instability in the GLC/NLC MDR with the simulation code HEAD-TAIL. In the field free regions of the MDR, a head-tail instability is observed to occur for an average electron-cloud density close to $2.0\text{E}+12 \text{ e/m}^3$, see Fig. 2, leading to a strong vertical emittance blow-up and particle loss. The growth time of the instability is in the order of 100 μsec . In particular, this electron-cloud density threshold occurs when the secondary electron yield at the wall exceeds $\delta_{\text{max}} \sim 1.5$ in the field-free regions. Study of the head-tail instability in the arc dipole and damping wiggler sections of both GLC/NLC and TESLA DR are underway. Simulations confirm that a slightly positive chromaticity or a larger synchrotron tune increase the threshold for the instability as expected but this is unlikely to provide the margin of safety that is desired.

Similarly, the code CLOUD_MAD has been used to estimate the single bunch thresholds in the positron transport lines of the BCS, the main linac, and the BDS. The electron cloud effects manifest in different ways in each of these different regions. For example, the thresholds for single-bunch emittance increase and beam size blow up in the BDS is $\sim 1.0\text{E}+11 \text{ e/m}^3$ [11] where the effect mainly arises from the mismatch of the optical functions due to the focusing from the electron cloud. Unfortunately, it is not possible to simply retune the BDS optics because the electron cloud density, and thus the focusing mismatch, changes along the bunch length. The thresholds in the main linac and the BCS are $\sim 5.0\text{E}+13 \text{ e/m}^3$ [12]. In the main linac and the bunch compressor pre-linac, the instability manifests itself by modulating the position within a single bunch while in the arcs of the bunch compressor the instability arises from a mismatch of the optical functions much like that in the BDS.

Finally, the threshold for a coupled bunch instability in the GLC/NLC main damping ring is estimated for a cloud density $> 1.0\text{E}+13 \text{ e/m}^3$. Feedback may correct the coupled bunch instability at a growth time of 100 μs estimated for this density level. Coupled bunch instabilities have not been estimated for the transport lines but are not expected to be a limitation.

1.1.5 Remedies for the electron-cloud build-up

The SEY for *as received* aluminum vacuum chamber material is unacceptably high for both machines damping ring designs. Thus, we are planning to coat the aluminum vacuum chamber. An experimental program is well developed at SLAC, to measure the secondary yield of TiN and TiZrV thin film coating materials and the reduction of the SEY due to electron bombardment or ion sputtering. The non-evaporable TiZrV getter material provides pumping after its activation; activation is obtained by means of heating which reduces also the SEY.

The electron bombardment, so called conditioning or scrubbing effect, is effective in reducing the SEY of technical vacuum chamber materials. The peak SEY of TiN is reduced below 1.2 by applying an electron dose of $\sim 0.5 \text{ mC/mm}^2$. In the case of TiZrV material, an order of magnitude larger electron dose is needed to reduce the secondary yield to the same value. Recontamination of the material under vacuum results in an increase of the SEY; this effect is still under study.

The electron wall current of the cloud itself will provide the necessary conditioning. Assuming nominal GLC/NLC MDR beam parameters, the estimated

average electron-cloud current hitting the surface of the vacuum chamber is $0.5\mu\text{A}/\text{mm}^2$. At the initial stage of machine operations it will be necessary to run with lower beam intensity. When operating the MDR with a beam current just above the threshold to develop electron-cloud for conditioning purpose, but below the threshold for head-tail, simulations estimate an electron wall current of $2.5\text{nA}/\text{mm}^2$. Thus, ramping the beam current up, the required electron conditioning dose may be achieved in $\sim 2.0\text{E}+05$ sec or during few tenth hours of beam operation in the commissioning period.

Concern has been expressed [13] about the possibility that TiN coating materials may evaporate in time under continuous machine operations, i.e. photons, ions and electrons hitting and degrading the surface coatings. The issue needs to be addressed.

A promising remedy is given by fabricating the vacuum chamber surface with a particular design profile. We have studied the secondary electron emission from a metal surface with a grooved triangular and rectangular design profile [14,15]. Secondary electrons emitted from the grooved surface are likely to hit other wall of the groove causing a partial trapping of electrons which results in a suppression of the effective secondary emission yield (SEY). Thus, the special groove design is expected to reduce the escape probability of electrons in the proximity of the surface, reducing considerably the effective SEY at the surface. Analytic estimates [15] show that a SEY reduction by a factor ~ 2 is achieved with a groove angle design of 40° . The proposed mechanism of SEY reduction might be important for suppression of the electron-cloud effect in particle accelerators. Aluminum and copper samples with the special groove surface profile are being produced and measurements of the SEY are underway.

Among possible remedies we consider also solenoid windings. A longitudinal solenoid field of 10-20 Gauss has been extremely effective in reducing the electron cloud effect in the PEP-II and KEKB, with considerable enhancement of luminosity performance. Solenoid field is effective in field free regions. It may be applied in the BDS regions and a small fraction 15% of the GLC/NLC main damping ring. *In situ* ion sputtering is also under study.

As mentioned in section 1.1.3, simulations show that reduction of the SEY or increase of the chamber aperture in the BDS region, decrease the peak cloud density during a single bunch train pass. The 8 msec bunch spacing between trains should be sufficient for the electron-cloud to dissipate.

1.1.6 Miscellaneous discussions

We have estimated the equilibrium density level in both linear collider damping rings and the thresholds for the single- and coupled-bunch instability in the GLC/NLC main damping ring. Simulations indicate that a reduction of the secondary electron yield below a peak value of ~ 1.2 is required to avoid the electron-cloud effect in the damping wiggler sections of both damping rings. The electron-cloud effect is an issue in the arc sections of both DRs.

To reduce the electron-cloud effect in the GLC/NLC, various possible remedies are meant to decrease the SEY to a value $\sim 1.1-1.2$ in a stable way.

Due to the estimated high electron wall current at the GLC/NLC main damping ring vacuum chamber, the required electron conditioning dose may be achieved in few hours of beam operations during the commissioning period.

To apply extra measure of security, we are developing a metal surface with a special groove profile design, which is estimated to reduce the secondary yield by a factor 2 from an initial value 2.0 to ~1.1. The groove profile design under study is expected to be effective mainly in field free regions.

Solenoid windings are effective in reducing the effect in the GLC/NLC beam delivery system and bunch compressor system and in a fraction of the main damping ring. Increasing the chamber aperture is beneficial in reducing the cloud density in the beam delivery system.

We are particularly grateful to our colleagues for many stimulating discussions, especially to R. Kirby, F. Le Pimpec, A. Wolski, K. Kennedy and G. Stupakov. We are grateful to NERSC for supercomputer support.

References

1. For an updated summary and links on electron cloud studies, see E-CLOUD02: <http://slap.cern.ch/collective/ecloud02/>. See also the upcoming E-CLOUD04 workshop to be held on April 2004: <http://icfa-ecloud04.web.cern.ch/icfa-ecloud04/>.
2. ILC-TRC Report 2003: <http://www.slac.stanford.edu/xorg/ilc-trc/2002/2002/report/03rep.htm>
3. M. A. Furman and G. R. Lambertson, "The Electron-Cloud Instability in the Arcs of the PEP-II Positron Ring," LBNL-41123/CBP Note-246, PEP-II AP Note AP 97.27, 1997.
4. F. Zimmermann and G. Rumolo, "Electron Cloud Simulation: Build Up and Related Effects," in *Proceedings of the Mini-Workshop on Electron-Cloud Simulations for Proton and Positron Beams, CERN Geneva, 2002* [Yellow Report No. CERN-2002-001 (unpublished)], p. 97.
5. CLOUD_MAD, T. Raubenheimer reference page http://www-project.slac.stanford.edu/lc/local/AccelPhysics/Codes/Ion_MAD-Cloud_Mad/dbates/nlc_cloudmadtools_doc/cloud_mad/index.html
6. F. Zimmermann, "CLIC Damping Ring," LC02 Workshop at SLAC, Menlo Park, CA, US, February 4-8, 2002. <http://www-conf.slac.stanford.edu/lc02/wg1/schedule.html>.
7. A. Wolski and M. Woodley, "The NLC Main Damping Ring Lattice" NLC LCC-0113, LBNL CBP Tech Note-276, February 2003.
8. R. Brinkmann, K. Flöttmann, J. Roßbach, P. Schmüser, N. Walker, H. Weise "TESLA Technical design Report," March 2001.
9. M. A. Furman and M. T. F. Pivi "Probabilistic model for the simulation of secondary electron emission" Physical Review Special Topic AB, Volume 5, 124404 (2002).
10. M. Pivi, T. O. Raubenheimer and M. A. Furman "Recent Electron Cloud Simulation Results for the NLC and for the TESLA Linear Colliders" in the Proceedings for the Particle Accelerator Conference PAC 2003, Portland, Oregon, US, May 12-16, 2003.
11. D. Chen, et al, "Single Bunch Electron Cloud Effects in the NLC Beam Delivery System," NLC LCC-0126, September 2003.

12. D. Chen, et al, "Single Bunch Electron Cloud Effects in the NLC Bunch Compressor System," NLC LCC-0131, October 2003.
13. R. Kirby and A. Kulikov, SLAC, private communication, 2004.
14. A. Krasnov "Molecular pumping properties of the LHC arc beam pipe and effective secondary electron emission from Cu surface with artificial roughness", CERN LHC Project Report 671.
15. G. Stupakov and M. Pivi "Suppression of the effective SEY for a grooved metal surface" in preparation for the upcoming ELOUD04 workshop [1], and to be published as to be LCC Note <http://www-project.slac.stanford.edu/lc/ilc/TechNotes/LCCNotes/>

[lcc_notes_index.htm](#).

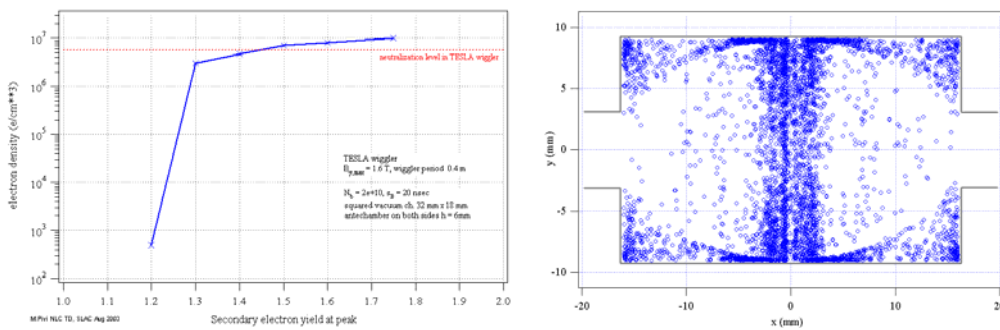


Figure 1. TESLA damping wiggler section. (Left) Equilibrium electron density as a function of peak SEY. Threshold for the development of the electron cloud is δ_{\max} $1.2 \div 1.3$. Note the neutralization level in the wiggler is high due to a small beam pipe cross section. (Right) Snapshot of the x- phase space distribution in the wiggler beam pipe, vertical stripes appear near the pipe center.

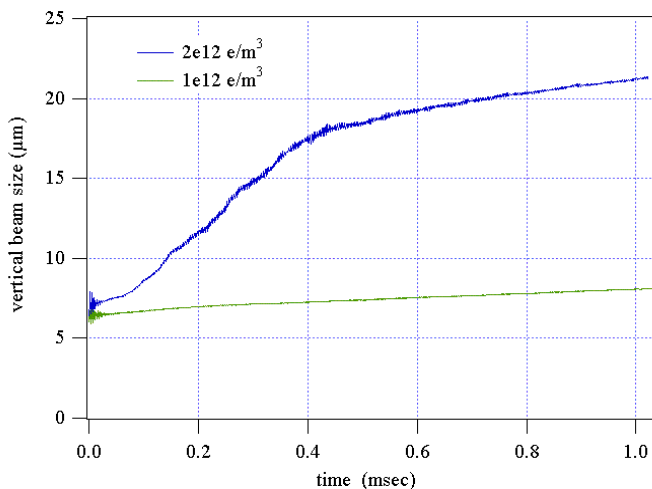


Figure 2. NLC MDR field free region. Time evolution of the vertical beam size, for different average electron-cloud density. A Single-bunch instability threshold appears for an electron cloud density close to $2.0 \times 10^{12} \text{ e}/\text{m}^3$.